Proceedings of the 1997 IEEE
International Conference on Robotics and Automation
Albuquerque, New Mexico - April 1997

Probabilistic Octree Modeling of a 3-D Dynamic Environment

P. Payeur†, P. Hébert†, D. Laurendeau†, C. M. Gosselin‡
Computer Vision and Digital Systems Laboratory
†Dept of Electrical and Computer Engineering
‡Dept of Mechanical Engineering
Laval University
Sainte-Foy, Québec, Canada, G1K 7P4
http://www.gel.ulaval.ca/~vision
[ppayeur, hebert, laurend, gosselin]@gel.ulaval.ca

Abstract

Probabilistic occupancy grids have proved to be very useful for workspace modeling in 2-D environments. Due to the formidable expansion of computational load, this approach was not tractable for mapping a 3-D environment in real applications. In this paper, the original occupancy grid scheme is revisited and a generic closed-form function is introduced to avoid numerical computation of probabilities for a range sensor with Gaussian error distribution. Occupancy probabilities are computed and stored in a multiresolution octree for improved performance and compactness. Occupancy models are built in local reference frames and linked to a global reference frame through uncertain spatial relationships that can be updated dynamically. This scheme is used for building a 3-D map in a telerobotic maintenance application of electric power lines where perturbations may cause motion of object assembly.

1 Introduction

The ability for modeling 3-D occupied and free space is a critical issue in robot reactive planning such as collision avoidance in cluttered workspaces. Occupancy grids offer interesting modeling characteristics since the 3-D space is tessellated into voxels whose occupancy state is measured directly from passive [9] or active range data [12], without the need for feature extraction. The resulting models are independent of the complexity of the scene geometry. Furthermore, occupancy grids provide a useful tool for collision detection.

Since data is of variable and limited precision when gathered from different ranges and viewpoints, an estimate of occupancy probability should be associated with every voxel in opposition to discrete grids that only provide *empty*, *occupied* or *unknown* states of the cells [2, 6, 8, 13]. This probabilistic information is helpful in finding next best views or secure free paths for robot guidance. For such low-level tasks, complementary representations based on geometrical models may not be necessary.

Elfes [3, 4] has initially proposed a framework for building 2-D occupancy maps of the environment of a mobile robot using a sensor error model in a Bayesian probabilistic approach to combine data from one or more viewpoints [10]. Although Elfes has brought some simplifications for applying this theoretical framework, the computational complexity of estimating the conditional probability of occupancy for every cell depends on the resolution of the map and increases exponentially with the number of cells. This leaves the method impractical for 3-D applications. To circumvent this problem, the Bayesian occupancy probability estimation procedure is revisited in the following and a closed-form approximation of the occupancy probability function for each new measurement allows for computational simplification which significantly speeds up the algorithm.

For 3-D space, the number of voxels in an occupancy map increases as a power of 3 with a resolution increase. However, several voxels may have a similar value for the occupancy probability and their state can thus be merged. Used as a multiresolution structure, the octree can improve the compacity of the model while allowing to incorporate information about the uncertainty (imprecision) of the state of each cell. It is thus proposed to encode occupancy probabilities of 3-D space maps into an octree structure to provide a detailed and compact model of the environment.

In this paper, the probabilistic octree framework is put to advantage for the development of a 3-D dynamic environment modeling system. The model is built from data provided by an active range camera from multiple viewpoints. The occupancy model is intended to serve as a map for guiding a telemanipulator in servicing on-line electricity distribution equipment.

Due to the oscillations produced by wind in outdoor scenes, a data gathering strategy for compensating perturbations is proposed to allow the construction of stable and unblurred models of 3-D environments. The scene is composed of one or more assemblies of rigid objects. To each of these assemblies is attached a local reference frame in which a probabilistic occupancy grid is built. These local reference frames are linked to a global reference frame through an uncertain spatial relationship.

0-7803-3612-7-4/97 $5.00 © 1997 IEEE

Section 2 extends Elfes' 2-D probabilistic mapping scheme to 3-D space and describes a framework for workspace modeling using probabilistic octrees. Section 3 describes the approximation of the occupancy probability function and section 4 details the integration of local grids into the global octree. Section 5 proposes a data gathering strategy under perturbed conditions. Finally, simulation results and performance considerations are presented for the power line maintenance application.

2 Occupancy grid framework revisited

Building a probabilistic occupancy grid model of a scene consists in estimating the probability that each cell is occupied based on sensor measurements. In the original framework proposed by Elfes [3], building such a grid involves two processing stages. First, a range measurement is interpreted using the probabilistic sensor model of the form $P[r|M]$ providing the probability of observing a measurement r given the actual state M of the grid. Secondly, the occupancy grid cell probabilities are updated using a Bayesian procedure.

Ideally, obtaining an optimal occupancy estimate of each cell in the first stage would require determining the conditional probabilities of all possible environment configurations. Even if the cell states are discretized to *empty* (EMP) and *occupied* (OCC) values, this leads to 2^n possible environment configurations in the 1-D case, 2^{n^2} configurations in the 2-D case, and 2^{n^3} configurations in the 3-D case for n cells along each axis of the grid. Currently, for a useful resolution level, the 3-D case is obviously not computationally tractable. To avoid this combinatorial explosion in the number of configurations, Elfes has assumed that the cell states are independent random variables. This is equivalent to assuming that the occupancy grid is a Markov Random Field (MRF) of order 0. This simplification implies that there are no causal relationships between the occupancy state of different cells. Experiments have shown that this assumption is acceptable for low-level robot guidance tasks. This simplification thus leads to a tractable evaluation of the probability that the state $s(C_i)$ of a cell C_i is occupied given a sensor reading r, $P[s(Ci) = OCC|r]$, using Bayes theorem and the probability density function of the sensor $P[r|M]$, as follows:

$$P\left[s\left(C_i\right) = OCC|r\right] = \frac{P\left[r|s\left(C_i\right) = OCC\right] \cdot P\left[s\left(C_i\right) = OCC\right]}{\sum_{s\left(C_i\right) = \{OCC, EMP\}} P\left[r|s\left(C_i\right)\right] \cdot P\left[s\left(C_i\right)\right]} \quad (1)$$

where

$$P\left[r|s\left(C_i\right) = OCC\right] = \sum_{\{G_{s\left(C_i\right)}\}} P\left[r|s\left(C_i\right) = OCC, G_{s\left(C_i\right)}\right] \cdot P\left[G_{s\left(C_i\right)}|s\left(C_i\right) = OCC\right] \quad (2)$$

for a specific grid configuration $G_{s(C_i)} = (s(C_1) = s_1, \ldots, s(C_{i-1}) = s_{i-1}, s(C_{i+1}) = s_{i+1}, \ldots, s(C_n) = s_n)$ in the set of all grid configurations $\{G_{s(C_i)}\}$ given that $s(C_i)$ is occupied. In the same way, equation (2) can be rewritten for $P[r|s(C_i) = EMP]$.

In spite of the assumption of independent random variables made by Elfes, equation (2) reveals that the probabilistic density function of the sensor must be evaluated for the entire set of configurations. For a sensor having a probabilistic distribution only along the measurement axis, this algorithm effectively remains tractable. But for a range sensor having a 3-D Gaussian probabilistic distribution, i.e. with imprecision along the measurement axis as well as on the orientation of the laser beam, each neighboring cell around the measurement must be considered. The configuration set thus becomes very large and a rigorous application of the numerical computation procedure still leads to an impractical algorithm implementation.

In the following, it is proposed to eliminate the heavy computational task of equations (1) and (2) for estimating the sensor distribution function and the occupancy grid probability. The idea consists in developing a closed-form approximation of the characteristic occupancy probability distribution function (OPDF) which results from the numerical evaluation procedure proposed by Elfes. Working on range measurements, this approximated OPDF is used to compute the occupancy probability of a given volume of 3-D space centered on the sensor viewpoint. Since the range sensor inherently scans a spherical area around a center point, the occupancy probabilities are first stored in local spherical occupancy grids. A given grid corresponds to a given scanning viewpoint of the sensor. These spherical grids are next integrated into the global Cartesian occupancy grid which is then encoded as an octree. Figure 1 shows the algorithm block diagram.

The algorithm is thus a two-step procedure. The first step computes local spherical occupancy grids around each viewpoint. The second step provides the global octree encoded model by merging the local spherical grids.

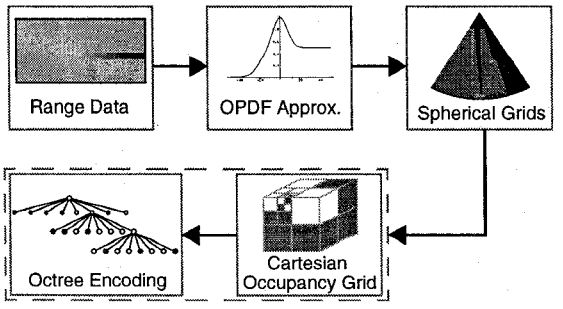

Figure 1 : *Integration algorithm of 3-D range data.*

3 Approximated probability distribution and local occupancy grids

The origin of the approximated OPDF is centered on the measurement $\boldsymbol{r}$ and shaped in accordance to the error distribution characterizing the sensor. It is parameterized along the axes following the alignment of the measurement axis.

For a sensor with Gaussian error distribution, the characteristic profile resulting from the occupancy probability estimation process proposed by Elfes has a shape which can be approximated by combining a sigmoid curve and a Gaussian-like function. The fitted curve exhibits a similar shape as the characteristic profile found by Elfes for a given value of the sensor's variance on range, σ_ρ^2. This is shown in Figure 2 for a one-dimensional probability distribution function. One must note that these curves are valid for a single measurement and each curve approximates the occupancy probability in space for this single range measurement with variance σ_ρ^2. The multiplicity of curves should not be confused with the updating process allowed by repetitive measurements as can be found in [3].

In Figure 2, the surface of the object is located at the transition point ($\rho = 50$ *mm*) while the sensor is at the origin. Far behind the object surface, the occupancy probability remains unknown ($P = 0.5$) while between the sensor and the surface it gradually drops to the empty state ($P = 0$).

For a generic sensor with two additional degrees of freedom including the azimuth (θ) and elevation (ϕ) angles, the closed-form approximation of the OPDF for a single measurement is expressed as follows:

$$P(\rho,\theta,\phi) = \frac{1}{2}\left(1+e^{-\left(\frac{2((\rho-\bar{\rho})+2\sigma_\rho)}{\sigma_\rho}+\frac{(\theta-\bar{\theta})^2}{\sigma_\theta^2}+\frac{(\phi-\bar{\phi})^2}{\sigma_\phi^2}\right)}\right)^{-1} + \frac{1}{3}\cdot e^{-\left(\frac{(\rho-\bar{\rho})^2}{\sigma_\rho^2}+\frac{(\theta-\bar{\theta})^2}{\sigma_\theta^2}+\frac{(\phi-\bar{\phi})^2}{\sigma_\phi^2}\right)} \quad (3)$$

The intrinsic parameters of this approximation are provided by the variance characterizing the sensor along each axis (σ_ρ^2, σ_θ^2, σ_ϕ^2). ($\bar{\rho}$, $\bar{\theta}$, $\bar{\phi}$) are the measurement coordinates. For more clarity, the two-degree-of-freedom example (ρ and θ) is illustrated in Figure 3. The probability distribution is shaped like a dome centered on the measurement ($\bar{x} = 35$ *mm*, $\bar{y} = 0$ *mm*). The resulting occupancy grid shape is related to the multidimensional Gaussian distribution of the sensor imprecision. Here,

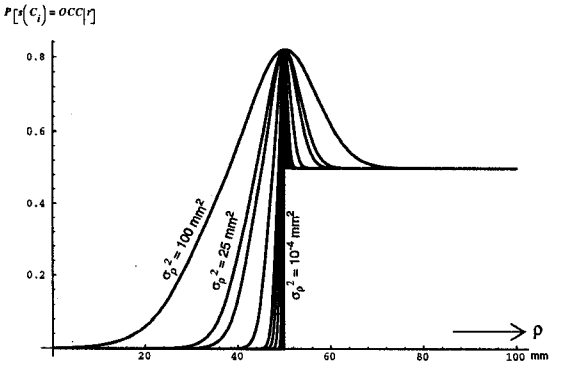

Figure 2 : *Approximated occupancy probability profiles for a single measurement with a sensor exhibiting Gaussian error distribution with parameters σ_ρ^2 varying between 10^{-4} mm^2 and 100 mm^2.*

variance parameters have been set to $\sigma_\rho^2 = 25mm^2$ and $\sigma_\theta^2 = 3x10^{-4}rd^2$ and the viewpoint is located at the origin.

Using such an approximation provides directly the probability that a cell is occupied for a given range measurement and avoids the heavy numerical computation of conditional probabilities. Moreover, the dependency on the discretization step along the sensor measurement axis, an artefact caused by the cell state independency assumption (0^{th} order of MRF), is eliminated since the approximation is continuous and can be evaluated everywhere along the measurement axis.

The approximated OPDF is computed for each measurement contained in one scan with given sensor parameters (σ_ρ^2, σ_θ^2, σ_ϕ^2) as shown in Figure 4a. The resulting occupancy probability distribution is temporarily stored into a spherical occupancy grid before being merged with the other occupancy probability distributions associated with the other measurements contained in the

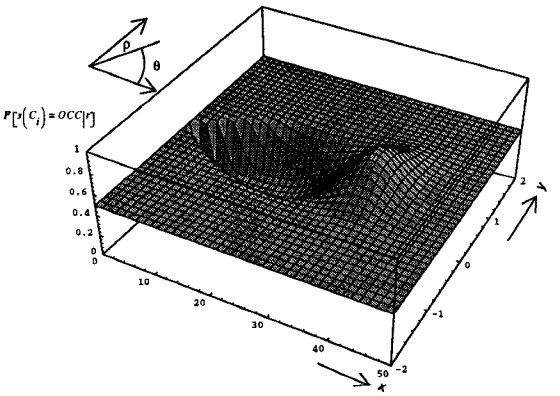

Figure 3 : *Approximated occupancy probability distribution function for one measurement from a two-degree-of-freedom sensor.*

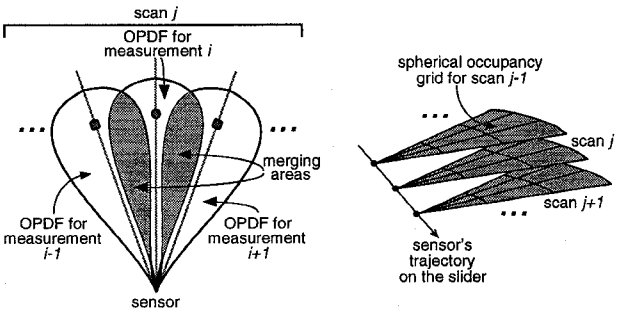

a) approximated OPDFs for 3 measurements

b) set of spherical occupancy grids

Figure 4 : *Approximated probability distribution merging process between each measurement and construction of local spherical occupancy grids for each scan.*

same scan. The merging process is performed using the following Bayesian rule:

$$P[s(C_i) = OCC|P_1, P_2] = \frac{P_1 P_2}{P_1 P_2 + (1-P_1)(1-P_2)} \quad (4)$$

where P_1 and P_2 are the respective occupancy probabilities of the occupancy grid cells that are merged together. This provides a local spherical occupancy grid containing the occupancy probabilities resulting from the entire set of measurements contained in one scan. The measurements are uniformly distributed on slices of the spherical grid. Figure 5 shows such a probabilistic spherical occupancy grid for one scan located at a given angle ϕ. White cells reveal a probability of occupancy close to one showing the objects surface while black cells represent empty space. Gray cells illustrate the unknown area located behind the objects surface. Gray cells also appear on each side of the scanned surfaces since the approximated OPDF affects both the cells located along the measurement axis and the neighboring ones. This results from the uncertainty on sensor orientation for each measurement of the scan.

In some circumstances, when safety considerations prevail on the representativity of the model, the Bayesian merging process may be replaced by a more conservative rule such as:

$$P[s(C_i) = OCC|P_1, P_2] = Max(P_1, P_2) \quad (5)$$

where the resulting occupancy probability is the maximum of the two probabilities (P_1, P_2) to be merged. This approach has been tested in the current application because collision avoidance with high voltage cables is of paramount importance.

This first computing step is repeated for each scan. For N scans gathered by the sensor, a set of N spherical occupancy grids is thus available for building the octree representation of the scene as shown in Figure 4b.

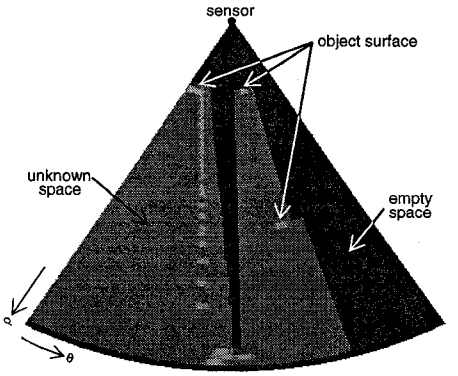

Figure 5 : *Spherical grid resulting from one scan composed of 128 range measurements (Resolution: 50 mm along ρ, $9x10^{-3}$ rd along θ).*

4 Probabilistic octree-based model building

Since the occupancy model of the scene has a cubic shape, each local spherical grid must thus be integrated into the global occupancy grid.

A first integration approach would be to scan each cell of the spherical occupancy grid and find the corresponding cells in the Cartesian grid to update their occupancy probability. However, since spherical cell boundaries do not coincide with Cartesian cells, interpolation techniques must be applied to avoid that the resulting model includes erroneous empty voxels.

Another approach could be to scan the entire workspace of the Cartesian occupancy grid subdivided to its higher resolution level. Each of the cubic cells must then be matched with their corresponding spherical cells to update the probabilistic occupancy state. But doing so reveals to be computationally expensive, especially for high resolutions. The number of cells Q to visit for an n-dimensional model is given by:

$$Q = \left\lceil \frac{ModelSize}{Resolution} \right\rceil^n \quad (6)$$

where *ModelSize* is the size of the entire model and *Resolution* is the size of the finest occupancy grid cell. Although working in 2-D space allows such a procedure, extending the technique to 3-D space is time consuming.

It is rather proposed to take advantage of the multiresolution property of octrees to avoid useless volume matching where no data had been gathered. Starting at the coarsest level of resolution, the approach consists in recursively checking whether a given cell of the Cartesian occupancy grid intersects with a given spherical occupancy grid. When the Cartesian voxel does not match any part of the spherical grid, it is discarded and its occupancy probability is left unchanged. On the other hand, when the spherical occupancy grid intersects with the voxel of

interest, the latest is subdivided into the next finer resolution level in the octree and the intersection test is repeated for each of the eight children which have just been created. This process is repeated until the highest level of resolution is reached. To speed up the algorithm, intersection checking is based on a progressive refinement such that the fastest parts of the test are made first. Vertices of the spherical occupancy grid are precomputed to speed up the procedure.

The Cartesian cells that are matched with a corresponding spherical cell have their occupancy probability updated following a Bayesian rule such as equation (4). Here P_1 corresponds to the current occupancy probability value of the voxel already stored in the octree. This probability is initially set to 0.5 (*unknown*) for a new model. P_2 is the maximum probability of the spherical grid cells that intersect the voxel. Coordinates of the eight corners and of the center point of the voxel are considered to evaluate this maximum probability. Using only the probability of the center point of the voxel to update the occupancy probability brings some incoherent data into the model since a cubic voxel does not necessarily lie entirely inside a single cell of the spherical grid. Using the maximum occupancy probability value of the voxel overrides this problem and ensures a safer model.

In the current implementation, local spherical occupancy grids are built sequentially before being integrated one at a time into the global Cartesian octree-based model. However, since each spherical grid is independent from the others, the scalability of the procedure for parallel implementation is high. Intersection checking, which is the most demanding part of the algorithm, can even be processed simultaneously on multiple spherical grids.

Our approach thus differs from Elfes' in that it avoids the use of discrete configuration sets of the grid to estimate the occupancy probability. With the closed-form approximation of the occupancy probability distribution, the computation is entirely analytic. Furthermore, instead of resampling the entire occupancy grid to transform the spherical grid into the Cartesian grid, advantage is taken of the multiresolution property of the octree. This allows processing large volumes of space in a single step thus speeding up the algorithm. Figure 6 shows a comparative scheme of both approaches.

5 Data gathering in a dynamic environment

To build and maintain an occupancy model in actual operating conditions where perturbations may occur, one must compensate for the relative motion between the sensor and the scene. Otherwise, the recovered model would be blurred and useless, especially for robot guidance. In the power line maintenance application, sensors are mounted on a working platform at the extremity of a truck boom. While the working platform is exposed to vibrations, the rigid assembly composed of the pole, the crossarm, the insulators and the conductors is also submitted to external perturbations such as wind for instance (see Figure 7).

One possible way to deal with this problem consists in using a set of cameras with synchronized shutters to grab instantaneously a snapshot of the whole scene of interest from different viewpoints [9]. However, significant development progresses are needed for this solution to become applicable.

A simpler solution that has been tested and adopted integrates a unique laser range sensor which can rotate (pan only) and translate on a slider mounted on the platform. The scanner grabs a profile in a very short period of time (< 0.1 *sec*) such that scan distortion due to motion remains

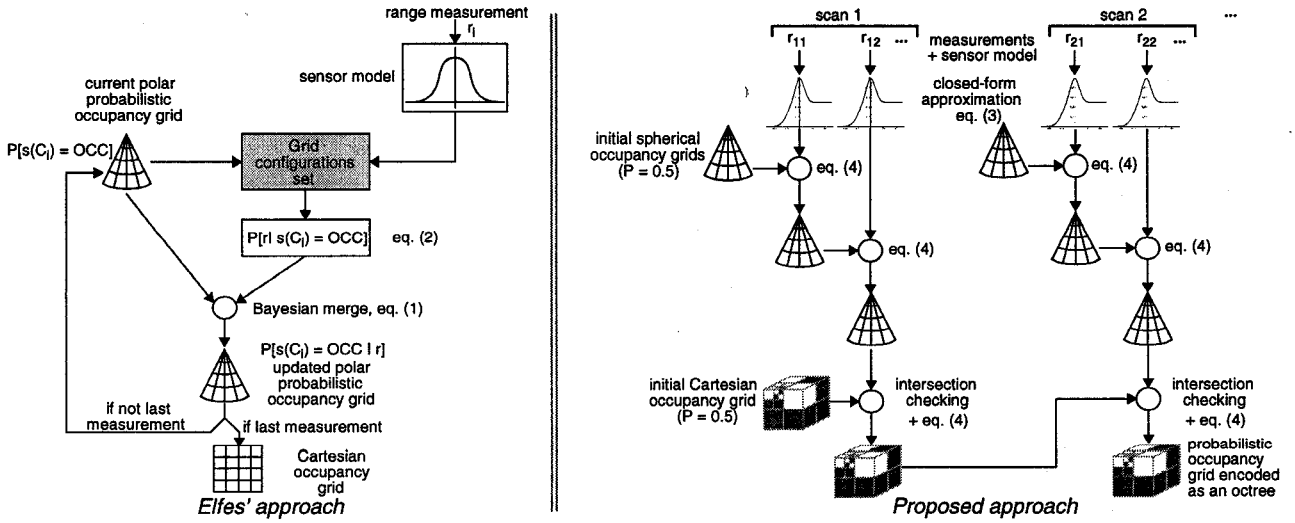

Figure 6 : *Comparative schemes of occupancy grid building frameworks.*

negligible. While grabbing scans, a small dedicated sensor, which is currently under development in our laboratory, acts as a high speed tracking device (HSTD) to keep track of the relative transformation between the platform and the scene.

Scans can then be transformed and integrated in the reference frame attached to the scene. Building the model in this local frame, only the transformation between the global reference frame, attached to the truck, and the scene reference frame has to be maintained during tracking. This eliminates the need to update the octree for moving objects [1, 11].

The HSTD consists of a video camera with a laser beam providing both an intensity image and a single range point. The camera is mounted on a fast orienting device [5] that tracks a reference point fixed at the extremity of the crossarm for instance. By calibration, the transformations between the HSTD (R_{hstd}), the platform ($R_{platform}$) and the range camera (R_{camera}) are obtained. The transformation between the HSTD and the scene is provided by the HSTD. These frames are depicted in Figure 7 showing a view of the workspace from the simulator. The manipulator which is usually located behind the slider is not shown for display purposes.

It is then possible to compute the transformation chain between the camera reference (R_{camera}) and the model reference frame associated with the target feature tracked by the HSTD (R_{scene}). Measurements $\boldsymbol{r}_{camera}$ are transformed from the range camera reference frame to the model reference frame as follows:

$$\boldsymbol{r}_{scene} = T_{hs}^{-1} T_{ph}^{-1} T_{pc} \boldsymbol{r}_{camera} \qquad (7)$$

where T_{hs}, T_{ph} and T_{pc} represent the homogeneous transformation matrices between the HSTD and the scene,

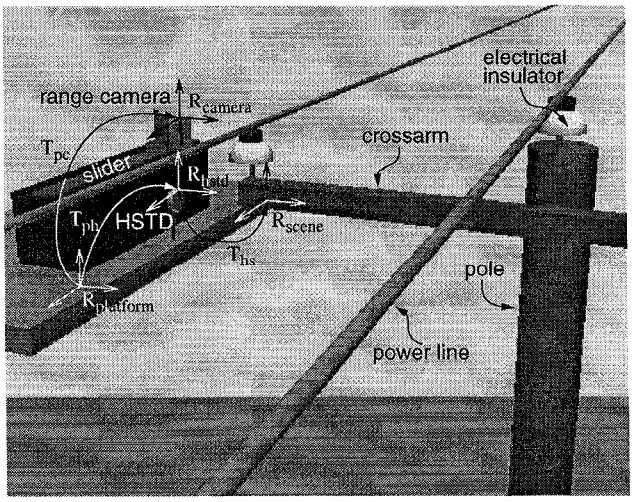

Figure 7 : *Workspace view and transformation chain for motion compensation.*

between the platform and the HSTD and between the platform and the camera respectively. $\boldsymbol{r}_{scene}$ and $\boldsymbol{r}_{camera}$ are the range measurements in the scene and in the camera reference frames respectively. Perturbations on the scene assembly or on the platform that may occur between two scans can be compensated within limits of precision of the transformation chain. When a robotic task has to be performed on a part of the moving scene, transformations provided by the HSTD are continuously used for controlling the robot by making it track the object on which the robot works.

6 Results and performances

To evaluate the performance of data gathering and integration procedure, a simulator has been developed for reproducing to scale an electric pole configuration and the sensing system mounted on the platform including the HSTD. The simulator processes are distributed over a network of workstations. A Silicon Graphics workstation is used for monitoring the simulation including the generation of perturbations of the platform and of an oscillatory motion to the pole for simulating wind effects. The workstation is also used as a graphic server for displaying the data gathering and the resulting models. A range sensor server runs on a Sun Sparc 4 workstation and provides range profiles from the current world state. Precision parameter for the range sensors were set to $\sigma_\rho^2 = 1mm^2$ and $\sigma_\theta^2 = 3x10^{-4} rd^2$.

Figure 8 shows the recovered model of the scene with the vertical pole, the crossarm, three insulators and conductors. Maximum resolution for a voxel was set to 50 *mm*. As a comparison, the length of the crossarm is 2.44 *m*. The range sensor gathered 320 scans from as many viewpoints on a trajectory where the sensor was pivoting and translating along the slider. Each scan contains 128 range measurements. The platform and the sensor faced the crossarm as illustrated in Figure 7. In Figure 8, gray shading of the cells corresponds to the probability of occupancy; white being 100% (*occupied*) and black 0% (*empty*). For the purpose of displaying the entire modeled volume, only voxels having a probability of occupancy higher than a threshold ε are displayed and unknown cells ($P = 0.5$) are removed. We can observe higher probabilities of occupancy for the extremity of the crossarm and the insulator that were closer to the sensor. Closer voxels' states are measured more often than farther ones, then their probability of occupancy converges toward 0 or 1 similarly to the Elfes' approach.

Simulation experiments have confirmed that the required computing time is directly related to the desired resolution and to the size of the scene area to model. For instance, computing a large model over 3 *m* such as in Figure 8 for a maximum resolution of 50 mm required less

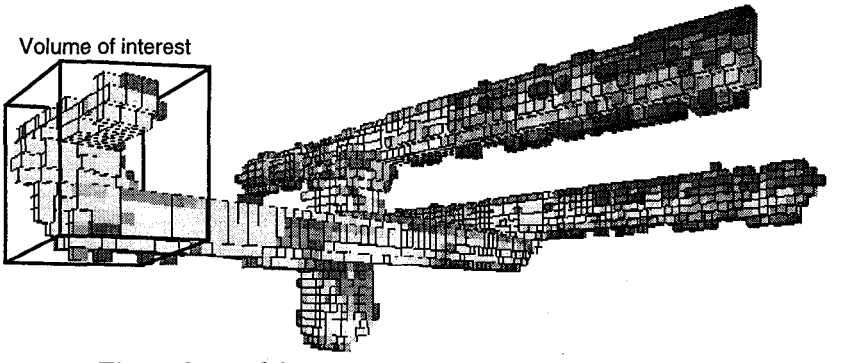

Figure 8 : *Model of the top of the pole (resolution: 50 mm).*

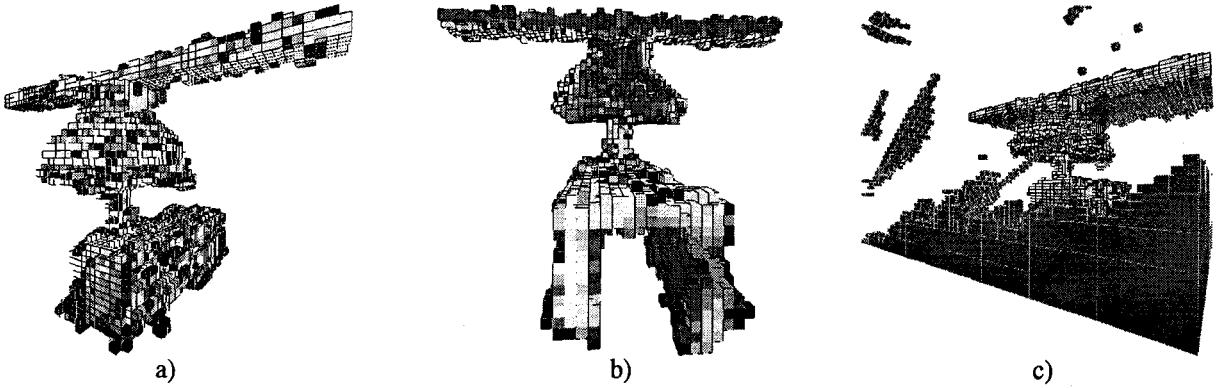

Figure 9 : *Models of the zone of interest (resolution: 10 mm).*

than 15 minutes on a Sun Sparc 4 workstation, while more than an hour was needed for a 10 *mm* resolution model. This suggests speeding up model building by focusing the modeled zone to a volume of interest in order to avoid high resolution integration of unneeded data. For instance, when scanning the electricity distribution pole, a coarse model of the scene is first built to prevent the manipulator from colliding with objects while acquiring further data. Then the human operator selects the volume of interest as a subregion of the coarse model corresponding to the area where a specific task must be achieved by the manipulator. Thereby, the integration algorithm rapidly eliminates irrelevant data.

Taking advantage of this strategy, models representing only one insulator and conductor, as well as the extremity of the crossarm have been computed with a 10 *mm* resolution. Figure 9 shows these models from different viewpoints. Each model can be computed in approximatively 10 minutes.

In Figure 9a and 9b unknown cells are not displayed. The center of the crossarm thus appears empty in b) where the model is observed from behind. This shows that the interior of objects keeps the 0.5 (*unknown*) probability level of occupancy in conformity with the probabilistic distribution function since these regions are located behind the surface captured by the range sensor. Figure 9c shows the same model but with the *unknown* cells displayed. Unscanned regions of the 3-D space appear as mean gray areas since they are still *unknown*.

For the simulations, the source of imprecision originated from the range sensor which was assumed to provide ρ and θ measurements following Gaussian distributions. However, imprecision may also originate from transformation errors occurring in the calibration process and from the transformation provided by the HSTD. The imprecision can be propagated through the compound transformations to estimate the precision of the sensor position. This can be done by linearizing the resulting transformation and developing the Jacobian matrix [14] or by applying the nonlinear transformation to sampled distribution of random variables and reestimating the distribution of the transformed samples [7]. In the 2-D case, Elfes proposed to convolve the occupancy grid with the probability distribution of the sensor position. This amounts to lessen sensor precision.

Figure 10 shows the resulting model of the insulator when the sensor error increases. The occupancy probability at the model surface is slightly lowered and distributed on a larger area as expected. It leads to a model with blurred surfaces. This result is not rigorously exact when rotation errors occur. This aspect might be investigated more deeply to reflect the actual imprecision caused by the transformation error.

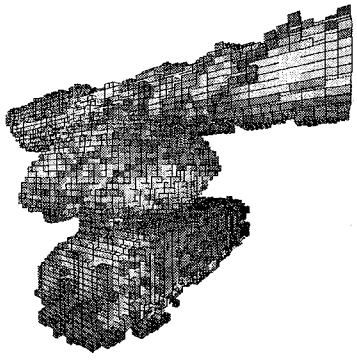

Figure 10 : *Effect of a loss of sensor precision.*

7 Concluding remarks

In this paper, probabilistic occupancy grids have been extended to the case of 3-D space modeling applications. Enhancements to the technique proposed by Elfes override the combinatorial explosion resulting from the addition of a third degree of freedom. The process makes use of a closed-form approximation of the probability distribution and takes advantage of the multiresolution characteristic of octrees to lead to a computationally tractable algorithm. However, simulation performances have shown that processing time must still be reduced significantly for acceptable performances in the maintenance task. This is achieved by locally controlling the bounding volume of the model as well as its resolution depending on the precision required for guiding the robot. Parallel implementation of the algorithm could also significantly reduce the computation time.

Another important point that was put forward in this work consists in maintaining one or several volumetric models in local scene reference frames while relating these frames to the global world system. In the electricity line maintenance task, the spatial relationship between the robot platform and the crossarm changes dynamically with perturbations. Using such a representation allows simple maintenance of the 3-D model since only one transformation is continuously updated. Furthermore, taking advantage of the high speed tracking device to update the reference frames relationship provides stable and unblurred models.

Acknowledgments

The authors are members of the Institute for Robotics and Intelligent Systems (IRIS) and wish to acknowledge the support of the Networks of Centres of Excellence Program of the Government of Canada, the Natural Sciences and Engineering Research Council (NSERC), and the participation of PRECARN Associates Inc.

References

[1] N. Ahuja and C. Nash, "Octree Representations of Moving Objects", *Computer Vision, Graphics and Image Processing*, 26(2):207–216, May 1984.

[2] C. I. Connolly, "Cumulative Generation of Octree Models from Range Data", In *Proceedings of the IEEE International Conference on Robotics*, pages 25–32, Atlanta, GA, March 13-15, 1984.

[3] A. Elfes, *Occupancy Grids: A Probabilistic Framework for Robot Perception and Navigation*, PhD thesis, Carnegie Mellon University, Pittsburgh, PA, 1989.

[4] A. Elfes, "Using Occupancy Grids for Mobile Robot Perception and Navigation", *IEEE Computer*, 22(6):46–57, June 1989.

[5] C. M. Gosselin and J.-F. Hamel, "The Agile Eye: A High-Performance Three-Degree-of-Freedom Camera-Orienting Device", In *Proceedings of the IEEE International Conference on Robotics and Automation*, pages 781–786, San Diego, CA, May 1994.

[6] R. Houde, J. Tremblay, F. Auclair and D. Laurendeau, "Pose Determination Using Octrees: A Comparative Survey", In *Proceedings of the Vision Interface Conference*, pages 220–227, Quebec, Canada, May 1995.

[7] S. Julier and J. Uhlmann, "A General Method for Approximating Nonlinear Transformations of Probability Distributions", Technical report, Robotics Research Group, Oxford University, 1994.

[8] D. Jung and K. K. Gupta, "Octree-based Hierarchical Distance Maps for Collision Detection", In *Proceedings of the IEEE International Conference on Robotics and Automation*, pages 454–459, Minneapolis, MN, April 1996.

[9] T. Kanade, A. Yoshida, K. Oda, H. Kano and M. Tanaka, "A Stereo Machine for Video-Rate Dense Depth Mapping and its New Applications", In *Proceedings of the IEEE 15th Computer Vision and Pattern Recognition Conference*, San Francisco, CA, 1996.

[10] H. P. Moravec, "Sensor Fusion in Certainty Grids for Mobile Robots", *AI Magazine*, 9(2):61–74, 1988.

[11] W. M. Osse and N. Ahuja, "Efficient Octree Representation of Moving Objects", In *Proceedings of the International Conference on Pattern Recognition*, volume 2, pages 821–823, Montreal, Canada, August 1984.

[12] M. Rioux, "Laser Rangefinders Based on Synchronized Scanning", *Applied Optics*, 23:3837–3844, 1985.

[13] Y. Roth-Tabak and R. Jain, "Building an Environment Model Using Depth Information", *IEEE Computer*, 22(6):85–90, June 1989.

[14] R. Smith, M. Self and P. Cheeseman, "Estimating Uncertain Spatial Relationships in Robotics", In I. J. Cox and G. T. Wilfong, editors, *Autonomous Robot Vehicles*, pages 167–193. Springer-Verlag, New York, 1990.